Thermal Science and Engineering Progress 54 (2024) 102849

Contents lists available at ScienceDirect

Thermal Science and Engineering Progress

journal homepage: www.sciencedirect.com/journal/thermal-science-and-engineering-progress

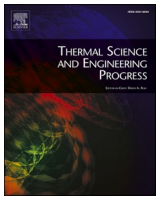

Experimental investigation of a new defrosting technique for sustainable refrigeration system

Burak Aktekeli [a,b,*], Mustafa Aktaş [c], Meltem Koşan [d], Yaren Güven [c], Erhan Arslan [e]

[a] Natural and Applied Science Institute, Gazi University, Ankara, Turkey
[b] Worker Health and Safety, Osmaneli Vocational School, Bilecik Şeyh Edebali University, Osmaneli, 11500 Bilecik, Turkey
[c] Energy Systems Engineering, Gazi University, Ankara, Turkey
[d] Energy Systems Engineering, Kahramanmaras Istiklal University, Kahramanmaras, Turkey
[e] TÜBİTAK Marmara Research Center, Gebze, Kocaeli, Turkey

ARTICLE INFO

Keywords:
Refrigeration
Defrosting
Solar energy
PVT collector

ABSTRACT

Defrosting can have a detrimental impact on the functioning of regularly used refrigeration systems. The primary objective of this study is to enhance the cooling efficiency by resolving the defrost process, which impacts the cooling performance due to the heat received from the system. A new solar PVT-assisted system, which includes a cold chamber, was created and tested for this specific purpose. Furthermore, a sophisticated automation scenario has been devised to function in five distinct modes, ensuring the successful execution of the defrost process. Two experiments, Experiment 1 and Experiment 2, were conducted. The average coefficient of performance (COP) and exergy values obtained were 2.29 and 2.25, and 25.74 % and 24.45 %, respectively. The maximum temperature change measured in the cold room during defrosting was 2 °C. In Experiment 1, the PVT collector produced a total energy of 2.85 kWh; Experiment 2 generated 2.79 kWh. Consequently, the defrosting procedure was effectively executed by directing hot air into the chilly chamber using the proposed sustainable method. This system is highly recommended because of its innovative defrosting mechanism, which guarantees optimal solar energy utilization.

1. Introduction

Today, the development of technology and the increase in population lead to a rise in global energy demand. Most of the energy needs are met by burning fossil fuels, and this causes severe damage. Countries are expected to switch from fossil fuels to more environmentally friendly options to achieve net zero carbon emissions. Solar energy has gained significant importance as it is a clean, accessible, and inexhaustible renewable energy source. Energy conservation is critical to reducing energy consumption and carbon emissions [1,2].

Freezing, the most common problem of evaporators, reduces the efficiency of refrigerating systems. The contact of hot and humid ambient air with the cold evaporator surface causes frost to form on the evaporator surface. A layer of ice/snow covers the evaporator surface and impairs heat transfer. As the frost thickness in the evaporator increases over time, the frost reduces the heat transfer process. It resists the airflow through the coil, reducing the evaporator's airflow. Accumulated frost increases the air-side thermal resistance and causes additional airflow resistance to build up. These factors reduce the heat transfer performance of the evaporator, resulting in a reduction in heating capacity and system efficiency. Frost significantly impacts operating performance and leads to additional energy consumption. As a net effect, both compressor uptime and energy consumption increase. Periodic defrosting is therefore necessary to maintain the required heating capacity and performance coefficient of the cycle. This ice-melting process is often called "defrosting" in the literature. The chosen defrost method (electrical resistance defrost, reverse cycle defrost, hot gas defrost, etc.), defrost time, and defrost interval are critical in keeping the refrigerated products within the desired temperature range and in the refrigerator's energy consumption. Defrosting melts snow/ice and cleans the evaporator surface, helping the refrigerating system to work efficiently. Failure to defrost can have several negative consequences. The layer of snow/ice covering the evaporator surface reduces heat transfer and refrigerating efficiency. This causes the refrigerating system to consume more energy, reducing the energy efficiency of the refrigerating system and increasing energy costs. Frost accumulated on the evaporator coil is usually periodically removed using electrical

* Corresponding authour.
E-mail address: burak.aktekeli@bilecik.edu.tr (B. Aktekeli).

https://doi.org/10.1016/j.tsep.2024.102849
Received 9 July 2024; Received in revised form 23 August 2024; Accepted 26 August 2024
Available online 28 August 2024

Nomenclature

A_c	Collector area (m^2)
AC	The profit from defrosting ($/year)
COP	Coefficient of performance
ET	The unit price of electricity ($/kWh)
$\dot{E}_{air}$	Energy of air (Watt)
$\dot{E}_{con}$	Condenser capacity (Watt)
$\dot{E}_{dc}$	Energy in drying chamber (Watt)
$\dot{E}_{el}$	Electrical energy (Watt)
$\dot{E}_{evap}$	Evaporator capacity (Watt)
$\dot{E}_{loss}$	Loss energy (Watt)
$\dot{E}_{solar}$	Energy from solar irradiation (Watt)
$\dot{E}_{ther}$	Thermal energy (Watt)
F_R	Heat removal efficiency factor
h	Heat transfer coefficient (W/m^2K)
I	Solar irradiation (W/m^2)
I_{PV}	Photovoltaic current (A)
L_{ice}	Melting latent heat of ice (kJ/kg)
$\dot{m}$	Mass flow rate (kg/s)
m_{ice}	Mass of ice (kg)
P	Pressure (kPa)
P_{def}	The defrosting power (W)
PP_{def}	The payback period for the defrosting method (year)
PV	Photovoltaic
PVT	Photovoltaic-thermal
Q_{def}	The energy required for defrosting (kWh)
Q_{hg}	The amount of energy consumed in the hot gas (kWh)
$\dot{Q}_{input}$	The amount of input energy (kW)
Q_{melt}	The amount of energy required to melt the ice (kW)
$Q_{resistance}$	The amount of energy consumed in the electrical resistance (kWh)
R	Universal gas constant (kJ/kg K)
T	Temperature (°C)
TIC	The total investment cost ($)
$t_{compressor,hg}$	Operating time of compressor (h)
t_{def}	The operating time for the defrosting process (h)
$t_{resistance}$	Operating time of resistance (h)
U_L	Total heat transfer coefficient (W/m^2K)
U_{PV}	Photovoltaic voltage (V)
$\dot{W}_{comp}$	Power of compressor (Watt)
$\dot{W}_{fan}$	Power of fan (Watt)
W_R	Total uncertainty
$\dot{W}_{resistance}$	Power of resistance (kW)

Symbols

$\eta_{defrost}$	Defrost efficiency (%)
η_{th}	Thermal Efficiency (%)
η_{PV}	PV efficiency (%)
τ	Glass cover transmissivity
ρ	Density (kg/m^3)
α	PV cell absorptivity
ϕCO_2	Amount of CO_2 emitted per hour (kg CO_2/h)
ψCO_2	Average CO_2 emissions during coal power generation (kg CO_2/kWh)

Subscripts

c	collector
con	condenser
$comp$	compressor
el	electrical
$evap$	evaporator
hg	hot gas
$ther$	thermal

resistances. However, electrical resistance and hot gas methods could be more efficient. These methods accelerate evaporator refreezing, increasing energy consumption [3,4,5,6].

Frost formation is one of the challenges faced in low weather. In the literature, there are several studies on defrosting the evaporator. Karaağaç et al. [6] developed a defrosting method for photovoltaic thermal (PVT) assisted refrigeration systems. The new evaporator design, there is new evaporator design has a refrigerant line inside the evaporator and a hot water line from PVT. In the experiments, the freezing that occurs in refrigerating systems was tested, and freezing was accelerated in the evaporator. They used 605 W of power for each defrost process and calculated the average defrosting time to be approximately 4 min. They found the average electrical efficiency of the PV module to be 13.6 % and the average overall efficiency to be 38 %. The coefficient of performance was calculated as 4.18, which increased by 9 % on average during defrost. They presented an alternative defrost method to prevent efficiency loss due to temperature rise and reduce energy consumption by refrigerating the PV module.

Malik et al. [7] investigated the frost detection and defrost method for refrigerators. This system consists of photoelectric sensing, capacitive sensing, and resistance heating techniques. With the frost sensor, frost formation on the evaporator surface is sensitively detected and measured. This system, detects frost formation, measures the frost thickness, and ensures defrost when the crucial frost thickness is reached. Yoon et al. [8], tried three different defrost heater control methods to optimize the cabin temperature during defrost process. All modes increased defrost efficiency by reducing the temperature rise in the cabin during the defrost process. The best performance was achieved individually in the vibrating mode; the temperature change remained at 5 °C at the cabinet, and defrost efficiency increased by 15 % compared to the reference values.

Yu et al. [9] designed and tested a solar photovoltaic direct drive cooling system for cooling electronic devices in Tianjin. In 7 h of operation with an average solar irradiation of 776.5 W/m^2, the system produced 1.81 kWh of electricity, and 24.9 % of this was consumed in the vapor compression cooling cycle. Klingebiel et al. [10] experimentally conducted the effectiveness of reverse cycle defrosting, electric heater defrosting, and hot brine deicing methods. The experiments were carried out in a refrigerator designed as a cold storage. All defrosting methods were examined in a single evaporator. As a result of the experiments, the reverse cycle defrosting method had the highest efficiency, with an efficiency rate of 56–61 %. The defrost efficiency of electric heater defrost and warm salt water defrost methods was 44–45 %. Miao et al. [11] proposed the temperature-humidity-image defrost control method to improve the defrost process. They made experimental comparisons of air source heat pumps with the traditional and proposed temperature–time methods and the proposed and temperature–time methods. Compared with the conventional method, it was observed that thanks to the proposed defrosting control strategy, delayed defrosting and unnecessary defrosting were effectively prevented, and defrosting energy consumption could be reduced by 10.6 % and 22.3 %, respectively.

In this study, a new system is presented that can provide the defrost process in the refrigerator integrated with the PVT solar collector by giving hot air from the PVT or condenser and a new airflow structure in the evaporator without heating the cold room during the defrost process

(without using the electrical resistance or hot gas method and without consuming additional energy). Thus, it is aimed to provide energy efficiency since no extra energy is used in the defrost process. The cold room design proposed in this study aims to increase the performance of the system's performance and minimize energy consumption during the defrost process. This study was carried out in line with its objectives as below:

- To minimize the temperature increase value of the refrigerated products during the defrost process and to provide heat for defrosting with solar energy,
- To design a sustainable refrigerator with PVT assisted and investigation of its 24-hour performance,
- Investigating the effects of the new generation air flow method of the solar-assisted, energy-storage refrigerator on the system,
- Introducing a new environmentally friendly solar-assisted refrigerator into the literature,
- To analyze the solar refrigerator's performance in refrigerating and defrosting processes.

The study's main objective is energy efficiency, and a new defrosting method for self-powered refrigerators integrated with solar energy has been scientifically constructed, designed, analyzed, and experimentally demonstrated. This study presents and analyzes a system that can provide defrosting and cooling with its resources. This new defrost method with PVT presents the temperature change inside the room during the defrosting process. This study presents the results of the new method developed from an energy and exergy perspective, and a compact PVT that can perform cooling and defrosting operations with a single system is designed. The main structure of this paper is depicted in Fig. 1.

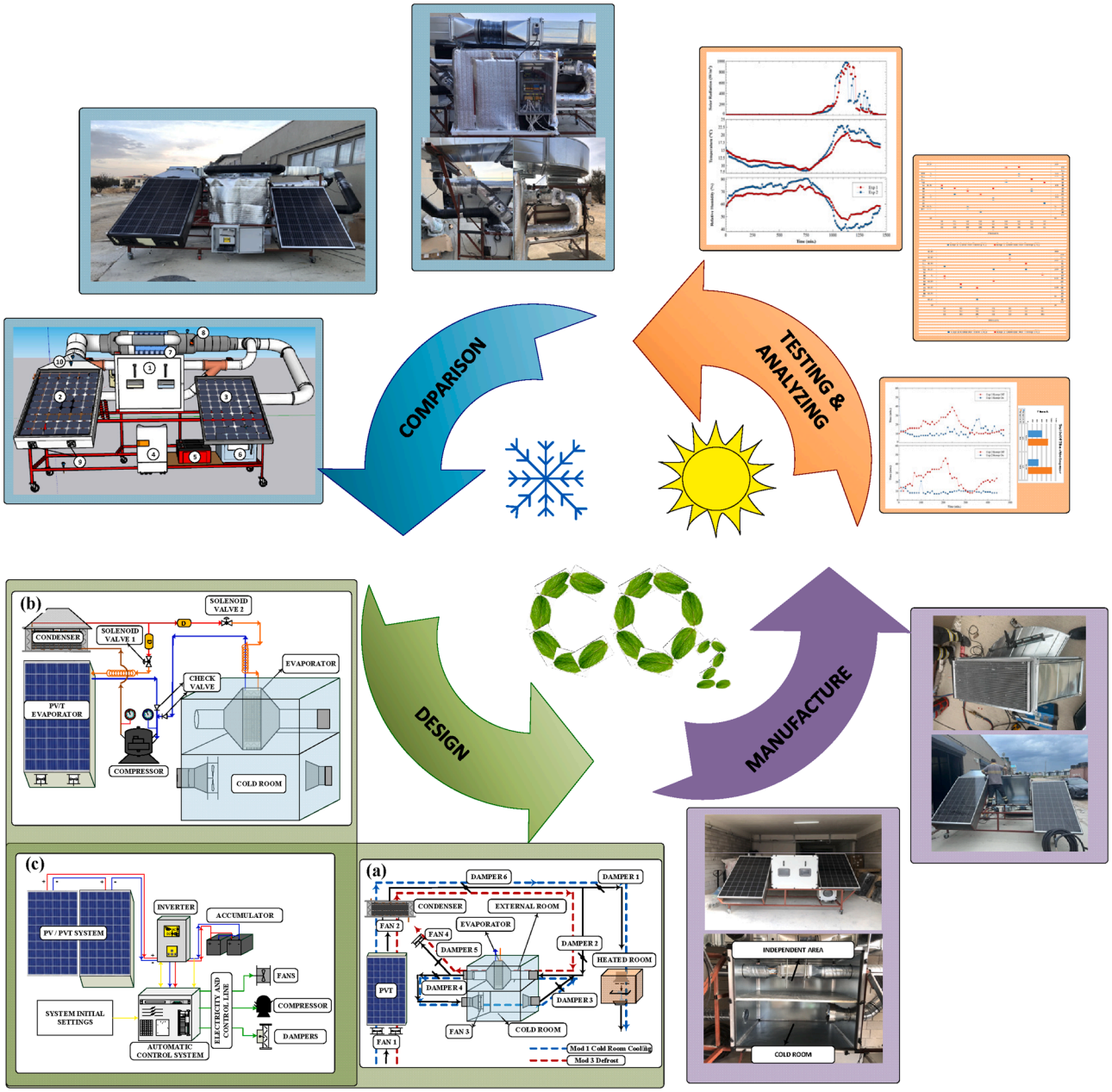

Fig. 1. Main steps of the study.

2. Material & methods

2.1. Design of system

This study aims to design a refrigerator with an innovative defrosting method as an alternative to hot gas and electric heater defrosting methods, with PVT and heat pump support. A special cold room design was made for this purpose. The cold room was made of aluminum sheet with 100 x 120 x 80 cm dimensions, with a total volume of 1 m3 and insulated with 50 mm glass wool. In this cold room, the evaporator and the cooled area were divided with a 20 mm sandwich panel to ensure sealing. In these two sections, the connections between the cold room and the evaporator were designed to be provided by air ducts and dampers connected to the ducts. The evaporator, which was placed in a separate part of the cold room from the cooled area, was designed to cool the cold room to the desired temperature when necessary, as well as to stop the airflow to the cold room by controlling the airflow with the control of the dampers during the defrost process. As a continuation of the defrosting process, hot air in the evaporator and ducts at the end of defrosting would reduce the quality of the cooled environment and increase energy consumption. It was considered to create an automation scenario to prevent the direct transmission of this hot air into the cold room. In this way, to avoid the deterioration of the air quality of the cooled environment, the compressor was activated at the end of defrosting and operated until the system entered the regime in the airflow during the defrosting process. Consequently, defrosting was achieved without heating the cold room with hot air from the PVT and heat pump. In this regard, the cold room was designed to provide synchronization by managing the air ducts and dampers with automatic control according to the PVT and heat pump integration. The automation scenario was based on 5 modes. These are cold room cooling mode (Mode 1), solar panel cooling mode (Mode 2), defrost mode (Mode 3), post-defrost standby mode (Mode 4), and standby mode (Mode 5). The system was designed to operate synchronously in 5 different modes to ensure the successful operation of this PVT and heat pump-assisted defrost structure.

Energy control in the system was made by the automation system and the smart inverter connected to the automation system. The system automation was programmed to store the electrical energy obtained from the PVT by the smart inverter when solar irradiation was present in two 160 Ah batteries and to use it for the system's needs when necessary. In addition, an automation system scenario was designed to meet the system's energy needs when solar irradiation was insufficient or absent with the energy stored in the batteries. It is known that as the PV panels in the system are cooled, their electrical efficiency increases. An integrated double evaporator design was realized, with one evaporator for cooling the PVT and the other evaporator for cooling the cold room. The priority in automation was the cooling of the cold room, and when the cold room reached the set value and the battery charge rate was 90 % and above, the PVT cooling system was activated, and a design for both cooling the PVT and storing the condenser waste heat in the phase change material was targeted. In the automation scenario, the compressor, solenoid valves, fans, and dampers were designed to be managed by automatic control depending on the system operating parameters, mainly the cold room cooling process, the defrost process, and the PVT cooling process depending on the battery charge rate and whether the targeted cold room set temperature value wa reached.

In the cold room, the indoor air temperature setpoint was entered into the automation system as + 4 °C and the compressor was turned off when the system reached the setpoint. In addition, since the temperature difference value of + 2 °C was entered into the automation system, the compressor was turned on again when the cold room air temperature value reached + 6 °C.

2.2. Description of the Experimental setup

The proposed design of the PVT-assisted refrigeration system is illustrated in Fig. 1. The system comprises a refrigeration cycle with a PVT collector, a cold room, a heat storage unit, and a heated room. The system has two evaporators: a PVT collector and a cold room. The copper pipes mounted in contact with the back surface of the PVT collector and the evaporator inside the cold room are the evaporators of the refrigeration system. In this design, the automation system is designed to activate both evaporators in different modes and at different times. To cool the PVT collector homogeneously and transfer the heat absorbed from the surface to the system, the PVT rear surface is filled with waste aluminum to contact the areas outside the copper pipes of the evaporator and the PVT rear surface. The heat load produced by this waste aluminum is transferred to the condenser with air. The condenser is positioned at the air outlet of the PVT. This way, the air passing through the condenser is sent to the system, increasing the heat load. The hot air sent to the system is stored in the heat storage unit for use. Phase change material is used in the heat storage unit.

In this design (Fig. 2), the PVT collector was cooled by both refrigerant and air. Two fans at the bottom of the PVT were used to deliver fresh air and the heat load in the PVT to the condenser. In addition, when the defrost process started at night when there was no solar irradiation, the evaporator of the cold room was disabled. The PVT evaporator was activated to obtain the hot air required for defrosting from the condenser. In this process, if the defrost air temperature obtained from the PVT collector is sufficient, the compressor remains in the off position, preventing the system from drawing excessive load, preventing excess energy consumption, and ensuring the system's sustainability by storing the system's energy. Hence, it was aimed to provide the heat required for defrost under all conditions, even in low weather conditions. The preheated air leaving the PVT was directed to three different purposes according to need: to the heat storage unit, to the heated room, and to the evaporator surface when the evaporator of the cold room needed defrosting. An energy storage unit has been designed stored to store thermal energy when solar irradiation is sufficient, and the system can operate sustainably with the stored energy when the irradiation is insufficient.

The evaporator in the cold room is positioned independently of the room. The cold room temperature was controlled by placing the channels and dampers connected to the channels at appropriate points. The defrost need of the evaporator of the cold room is programmed according to the compressor's operating time. When the defrost process begins, thanks to the automatic control of dampers and fans, the air inside the cold room is suppressed and the temperature fluctuation of the cold room is kept at a minimum level throughout the defrost process. In this way, a design that will prevent high energy costs by preventing the temperature of the cold room from rising and decreasing the environmental conditions and the quality of the products stored in the cold room has been presented in the literature. Additionally, a PV collector with the same characteristics was placed next to the PVT collector to evaluate and compare the electrical performance of this design. The airflow diagram, cooling system diagram, and electrical and automatic control details of the system are shown in Fig. 3.

In this study, a new system is presented that can provide the defrost process in the refrigerator integrated with the PVT solar collector by giving hot air from the PVT or condenser and a new airflow structure in the evaporator without heating the cold room during the defrost process (without using the electrical resistance or hot gas method and without consuming additional energy). Thus, it is aimed to provide energy efficiency since no extra energy is used in the defrost process. The new defrosting method was experimentally proven by testing for two days. Although solar energy is intermittent, the system presented worked with solar power for 24 h. The system has two modes: cooling and defrosting Fig. 3(a). Cooling and defrosting modes are characterized in this ecodesign based on minimizing the energy consumed and cooling the PVT

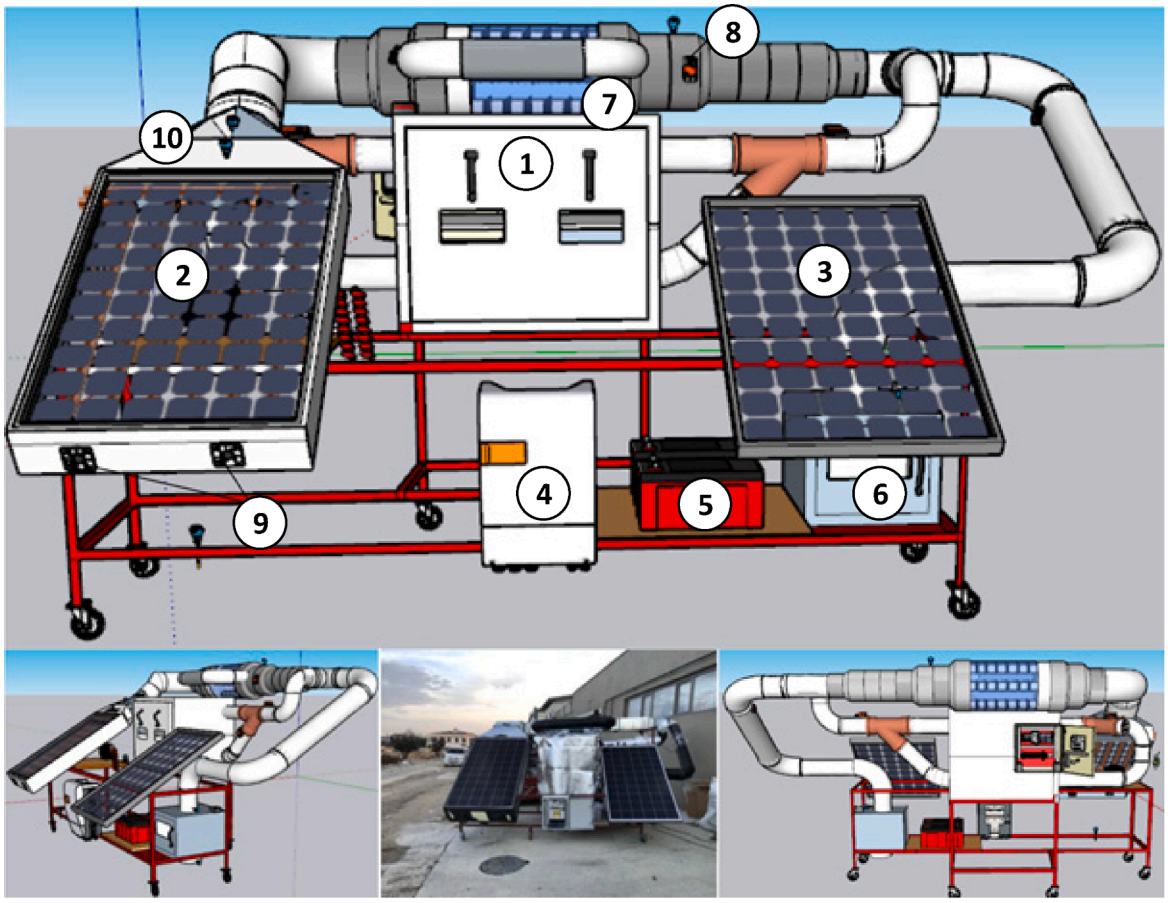

Fig. 2. A novel PVT collector refrigeration system.

and the room with a double evaporator Fig. 3(b). In cooling mode, the PVT is cooled when the battery is full, and the room is cooled with the electrical energy generated when the battery is empty Fig. 3(c). The heated room is heated with hot air. In defrost mode, the PVT and condenser operate to produce warm air. This solar-heated air is used for defrosting. Since the evaporator is outside the room, the room temperature remains low. With this system's new bifluid PVT structure, the air is heated, and the PV is cooled by the evaporator when needed. To increase the relative humidity level in the cold room, 12 bunches of approximately 3 kg of mint plants were washed and placed in the cold room for refrigeration application.

Fig. 4 shows a detailed view of the cold room. As seen in the figure, the cooled area is designed to be carried out in a section independent of the evaporator in the cooling system design. The 1 m^3 area is divided into two parts with insulated plates and impermeable materials. Cooling occurs in the lower chamber while the evaporator is placed in the upper chamber. The cooling system is designed for −10 °C evaporation and + 50 °C condensation temperature. Accordingly, while the temperature of the cold room was kept between + 4 °C and + 6 °C, the temperature on the evaporator surface varied between −4°C and −12 °C. Before starting both experiments, 12 mint bunches weighing approximately 3 kg were washed and placed in the cold room to prevent icing on the evaporator surface. This situation increased the icing on the evaporator surface and allowed the examination of the defrosting performance of the system.

Before the experiments started, the batteries in the system were first brought to 100 % charge level for both experiments. System equipment details are given in Table 1. In addition, the relative humidity level in the cold room was increased by placing a certain amount of vegetables in the cold room. Both experiments were conducted under the conditions prevalent in Ankara during November. The experiments started at 7:00p.m. and continued until 7:00p.m. of the next day after 24 h.

2.3. Automation scenario for experimental setup

The automation panel of the system was installed, and the automation scenario was designed to work in 5 modes. After pressing the F1 key for 2 s to turn on the system, the system counts down for 10 s to start up. At the end of the period, the system turns on and runs one of the modes depending on the system's state. A schematic representation of the automation scenario in this context is given in Fig. 5. Depending on the operating parameters of the system automation, transitions between modes were created as follows as a result of the analysis:

Cold room cooling mode (Mode 1): If there is no defrost and the room temperature is higher than the room set value (Room(°C) ≥ 6 °C), mode 1 will be activated.

Solar panel cooling mode (Mode 2): If there is no defrost, this mode will be activated if the cold room temperature is lower than the set value (4 °C≤Room(°C) < 6 °C) and the battery charge level is above 90 %.

Defrost mode (Mode 3): This mode will be activated unconditionally if the compressor operating time (60 min) exceeds the defrost time set value, that is, if the total time the compressor is in operation exceeds 60 min. 60 min was determined according to the principle of melting the ice that may form in the evaporator at the end of the compressor operating period.

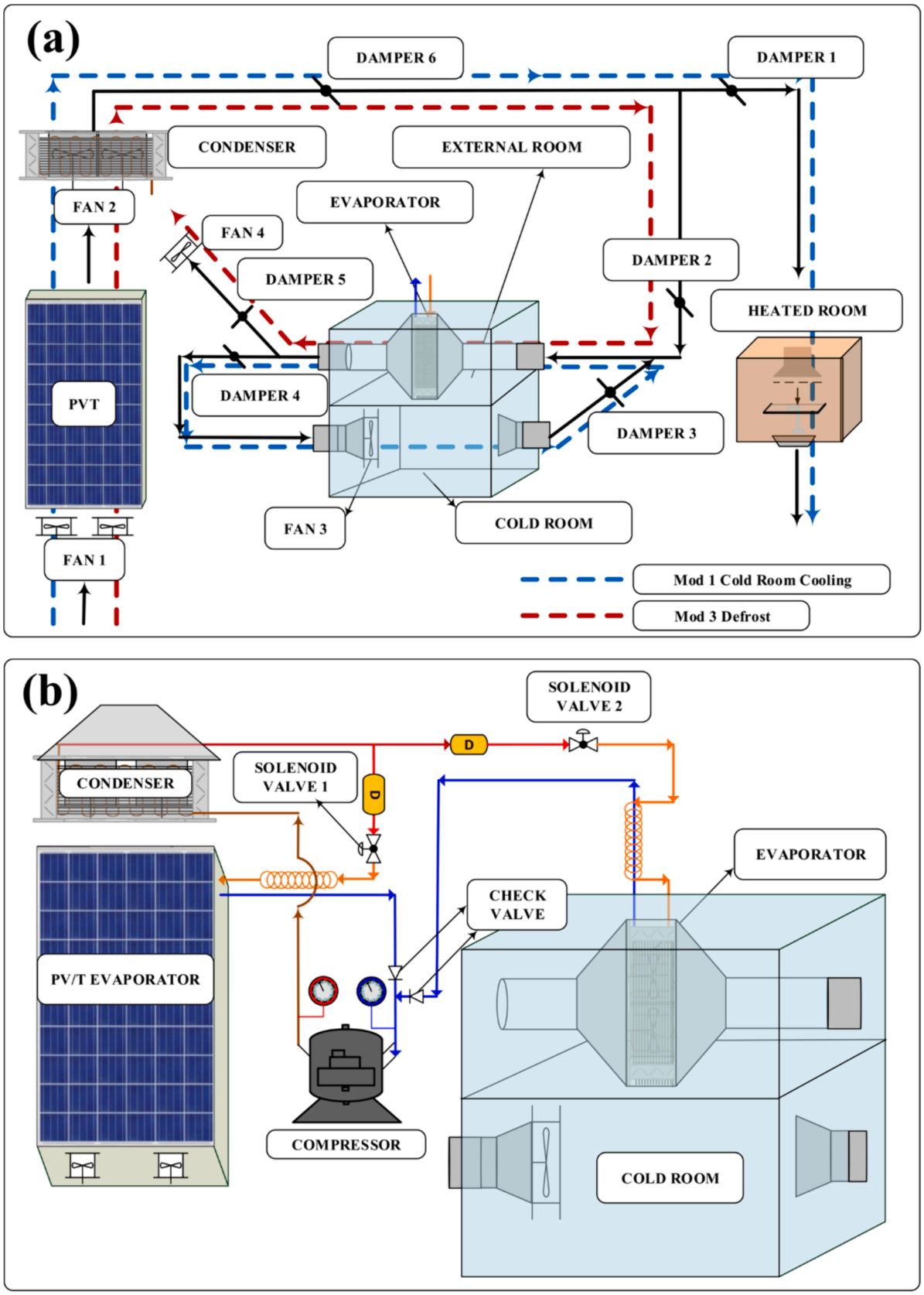

Fig. 3. (a) air flow diagram, (b) cooling system diagram, and (c) electrical and control diagram representation of the proposed system.

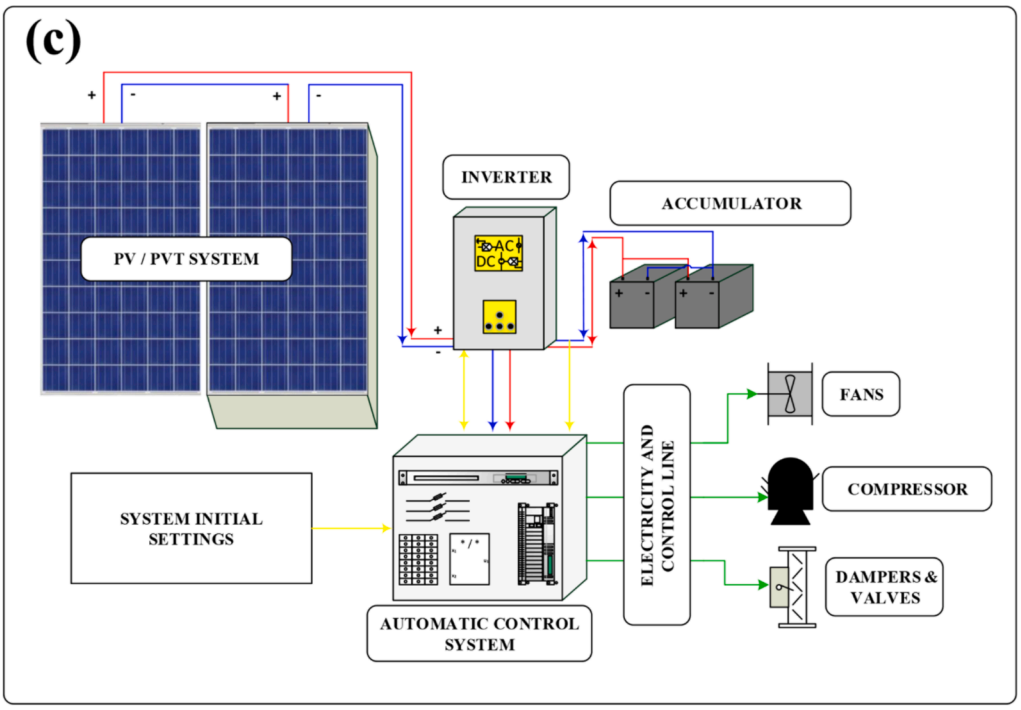

Fig. 3. (*continued*).

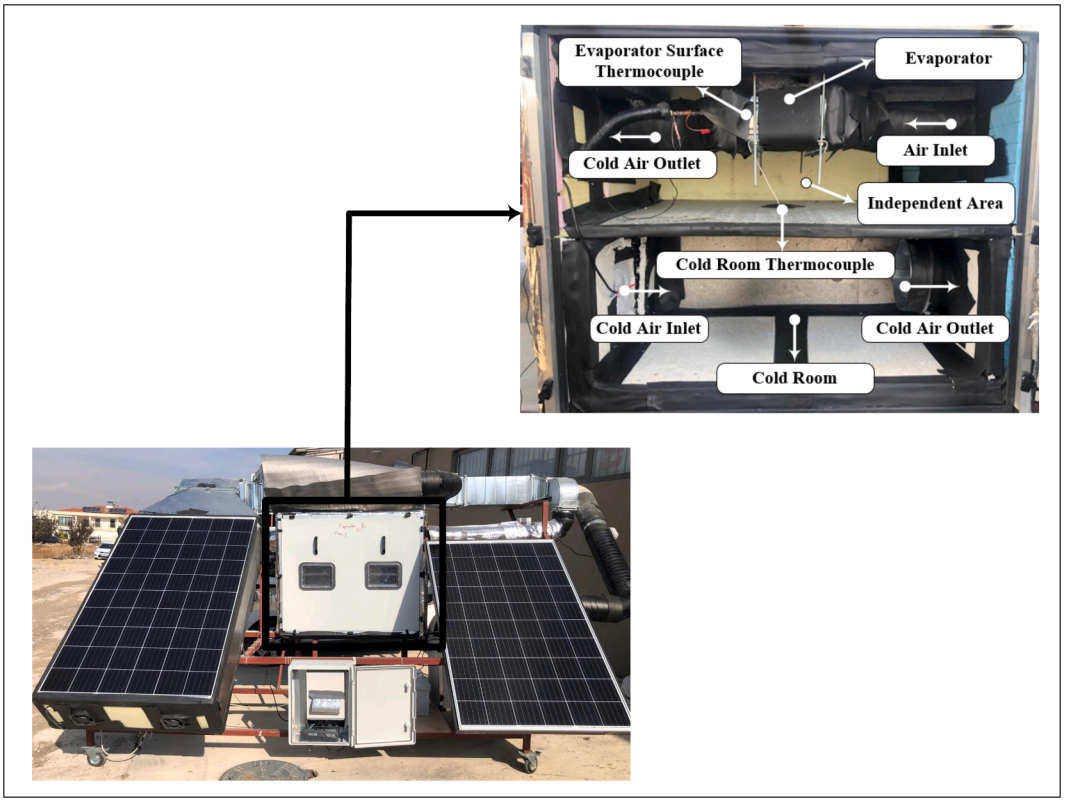

Fig. 4. The detailed view of the cold room.

Post-defrost standby mode (Mode 4): After the system terminates the defrost state, there is a 90-second waiting state, in this case, it prepares the system by positioning the appropriate dampers, and then the post-defrost mode comes into play, and the system must fulfill this state unconditionally after every defrost.

Stand-by mode (Mode 5): If there is no defrost, the cold room temperature is within the set value range or lower (4 °C≤Room(°C) < 6 °C), and the battery charge level is lower than 90 %, the system is ready in this mode waits.

The inside ambient air temperature set value in the cold room was

Table 1
Features of system equipments.

Equipment Name	Features
PV and PVT	Max. power 330 W Max. power voltage 33.80 V Max. power current 9.78A Tolerance ± 3 % 1669 mm*1002 mm*35 mm
Battery	12 V/160Ah/10HR Gel Accumulator
Fan 1	Voltage 220–240 V Power 22 W*2 = 44 W Operating frequency 50/60 Hz RPM 2850/3150 RPM
Fan 2	Voltage 220–240 V Power 10 W*2 = 20 W Operating frequency 50/60 Hz RPM 1000/1400 RPM
Fan 3, Fan 4	Voltage 220–240 V Power 16 W Operating frequency 50 Hz Flow 280 m^3/h
Haeted Room	50 mm sandwich panels insulated with glass wool 500*500*500 mm
Compressor	½ HP, R134a refrigerant, 330 W, displacement 14.28 cm^3
PVT Evaporator	3/8'' 11 m Internally Grooved Copper Tube is fixed in contact with the PV back surface. 1000 W
Evaporator	1000 W, Heat transfer surface area 2.27 m^2
Condenser	Microchannel Condenser, 1.79 HP, 1.335 kW,
Solenoid Valve	220 V, 20VA, −20 °C℃150 °C
Dumper motor	Voltage 100–240 V Operating frequency 50/60 Hz Power 1.6 W

entered into the automation system as + 4 °C, and when the system reached the set value, the compressor was off. In addition, the + 2 °C temperature differential value was entered into the automation system, so the compressor was activated again when the cold room air temperature value reached + 6 °C.

As shown in Fig. 5, the study is built on two basic system constructs: Cooling mode and defrost mode. While the system operates in cooling mode, the fresh air entering the PVT system absorbs the thermal energy obtained in the PVT. It draws some heat from the microchannel condenser integrated at the outlet of the PVT system, and the resulting hot air is transmitted to the hot room. Thus, an uninterrupted hot air flow required for the system is provided. When the compressor completes its operating time, the system switches to mode 3 defrost mode. The defrost is achieved by transferring the heat from PVT and heat pump to the hot air. To suppress the temperature rise of the cold room while defrosting with hot air, the evaporator is positioned in a section independent of the cooled environment created in the cold room. In this way, the hot air obtained from the system was discharged directly to the outside by passing over the surface of the evaporator, independently of the cold room, through the channels and the control of the dampers connected to the channels. In addition, if the charge rate of the batteries is above 90 % when the defrost process begins and there is a need for additional heat for PVT cooling or defrost air temperature, the system operates in PVT cooling mode. Following all defrost processes, thanks to the end-defrost mode, the dampers were kept fixed in the defrost position for 90 s to evacuate the hot air accumulated in the channels and on the evaporator surface, and the cold room evaporator entered the regime. Then, the dampers were placed appropriately to cool the cold room. Thus, the feasibility of a solar energy-assisted defrosting process that will keep temperature losses in the cold room at a minimum level has been experimentally proven.

The system heats the heated room in Mode 1 cooling mode. In Mode 3 defrost mode, it thaws the ice on the evaporator with the heat it receives from PVT and heat pump. During the defrosting process, since the evaporator was positioned in a section independent of the cooled environment in the cold room, the defrosting process was carried out by closing the airflow of the cold room through dampers and opening the dampers in the defrost line and passing hot air over the evaporator. During this process, the evaporator surface temperature and the time it takes for the dampers to reach the appropriate position during transitions between modes were also considered. The system, which exited the defrost mode and went into cooling mode, switched to Mode 4 end-of-defrost mode for the evaporator to reach the appropriate surface temperature for cooling and to evacuate the hot air in the defrost line, and after providing suitable conditions for cooling, it switched to Mode 1 cold room cooling mode. Thus, the conditioned air in the cold room is suppressed, and the temperature rise in the environment is kept to a minimum. This situation prevented the system's energy consumption and contributed to its sustainability.

2.4. Theoretical analysis

In this study, heat transfer fluids in PVT were bifluid as refrigerant and air. The energy from solar irradiation in PVT is provided as electricity, heat, and loss energy, and the energy balance in PVT is given below [12]:

$$\dot{E}_{solar} = \dot{E}_{el} + \dot{E}_{ther} + \dot{E}_{loss} \tag{1}$$

Where $\dot{E}_{solar}$, $\dot{E}_{el}$, and $\dot{E}_{ther}$ values are obtained as given in the equations below.

$$\dot{E}_{solar} = \tau.\alpha.I \tag{2}$$

$$\dot{E}_{el} = I_{PV}.U_{PV} \tag{3}$$

$$\dot{E}_{ther} = \dot{E}_{evap} + \dot{E}_{air} \tag{4}$$

In Eq. (2), τ is the glass cover transmissivity, α is the PV cell absorptivity, and I is the incident irradiation rate. Also, U_{PV} and I_{PV} refer to the voltage and current of the PV panel. The microchannel condenser is integrated into the output of the PVT. In this way, the energy equation in the condenser ($\dot{E}_{con}$) is the sum of the thermal energy ($\dot{E}_{ther}$) obtained from the PVT evaporator and the power of the compressor ($\dot{W}_{comp}$).

$$\dot{E}_{con} = \dot{E}_{ther} + \dot{W}_{comp} \tag{5}$$

$\dot{E}_{air}$, the energy obtained by cooling the PVT collector with air can be expressed [13]. In this equation, F_R, A_c, U_L, T_f and T_a mean heat removal efficiency factor, collector area, total heat transfer coefficient, average air temperature and ambient temperature, respectively.

$$\dot{E}_{air} = F_R.A_c\left[I.(\tau.\alpha) - U_L.(T_f - T_a)\right] \tag{6}$$

$\dot{E}_{evap}$, the energy absorbed by the refrigerant in the evaporator can be thermodynamically described as [14]:

$\dot{E}_{evap} = \dot{m}_r.(h_{evap,o} - h_{evap,i})$ (7) The energy equation in the condenser ($\dot{E}_{con}$) can be explained as:

$$\dot{E}_{con} = \dot{m}_r.(h_{con,i} - h_{con,o}) = \dot{m}_{air}.c_{p,air}.(T_{con,o} - T_a) \tag{8}$$

Here, $\dot{m}_r$ is the flow rate of the refrigerant and h is the enthalpy. The mass flow rate ($\dot{m}_{air}$) of the second fluid air used to cool the PVT collector can be calculated as [15]:

$$\dot{m}_{air} = \rho_{air}.V_{air}.A_{air} \tag{9}$$

$$\rho_{air} = P/R.(T_a + 273.15) \tag{10}$$

$$c_{p,air} = 1009.26 - 0.0040403T_a + 0.00061759T_a^{\,2} - 0.0000004097T_a^{\,3} \tag{11}$$

In Eq. (10) and Eq. (11), ρ_{air} is the air density, and $c_{p,air}$ is the specific heat of air. Here, P, R and T_a refer to pressure, gas constant, and ambient temperature. Thermodynamically, the equation of the energy

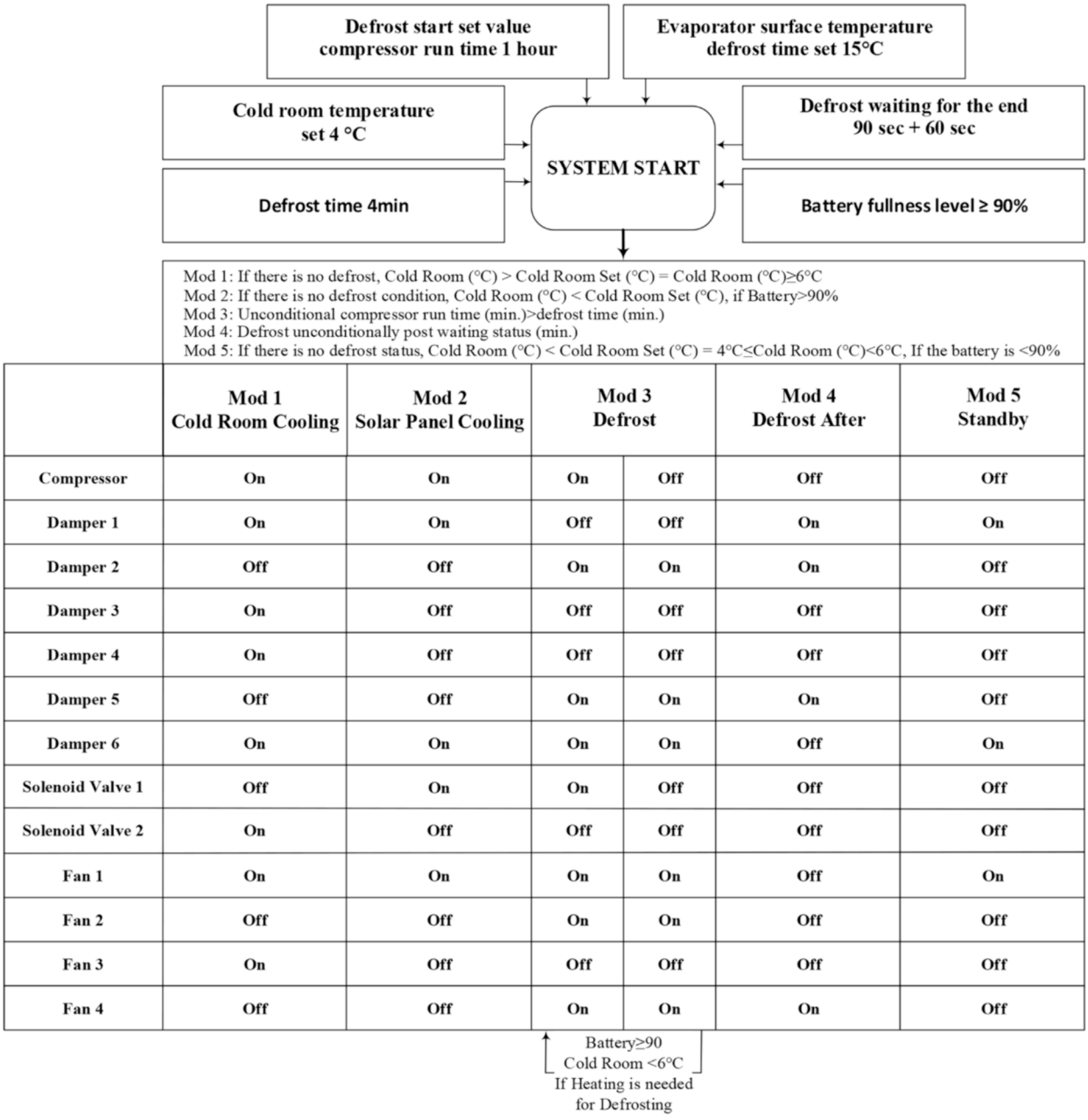

	Mod 1 Cold Room Cooling	Mod 2 Solar Panel Cooling	Mod 3 Defrost		Mod 4 Defrost After	Mod 5 Standby
Compressor	On	On	On	Off	Off	Off
Damper 1	On	On	Off	Off	On	On
Damper 2	Off	Off	On	On	On	Off
Damper 3	On	Off	Off	Off	Off	Off
Damper 4	On	Off	Off	Off	Off	Off
Damper 5	Off	Off	On	On	On	Off
Damper 6	On	On	On	On	Off	On
Solenoid Valve 1	Off	On	On	Off	Off	Off
Solenoid Valve 2	On	Off	Off	Off	Off	Off
Fan 1	On	On	On	On	Off	On
Fan 2	Off	Off	On	On	Off	Off
Fan 3	On	Off	Off	Off	Off	Off
Fan 4	Off	Off	On	On	On	Off

Fig. 5. System automation diagram.

consumption of the compressor ($\dot{W}_{comp}$) in the refrigeration system is expressed as follows:

$$\dot{W}_{comp} = \dot{m}_r.(h_{con,i} - h_{evap,o}) \tag{12}$$

The COP indicator, which determines the performance coefficient of the refrigeration system, is obtained as follows:

$$COP_{hp} = \frac{\dot{Q}_{con}}{\dot{W}_{comp}} \tag{13}$$

The thermal and electrical efficiencies of the PVT collector can be obtained as [16]:

$$\eta_{th} = \frac{\dot{E}_{ther}}{IA_c} \tag{14}$$

$$\eta_{PV} = \frac{\dot{E}_{el}}{IA_c} \tag{15}$$

Defrost efficiency is found in the following equation:

$$\eta_{defrost} = \frac{Q_{melt}}{\sum \dot{Q}_{input}} \tag{16}$$

The following equations describe the defrost efficiency obtained from electrical resistance and hot gas tests, respectively [17].

$$\eta_{defrost} = \frac{m_{ice}.L_{ice}}{Q_{resistance}} \tag{17}$$

$$\eta_{defrost} = \frac{m_{ice}.L_{ice}}{Q_{hg}} \tag{18}$$

Q_{melt} indicates the amount of energy required to melt the ice. In contrast,

$Q_{resistance}$ and Q_{hg} indicate the energy consumed in the defrost method with electrical resistance and hot gas, respectively [18].

$$Q_{melt} = m_{ice}.L_{ice} \tag{19}$$

$$Q_{resistance} = \dot{W}_{resistance}.t_{resistance} \tag{20}$$

$$Q_{hg} = \dot{W}_{compressor}.t_{compressor,hg} \tag{21}$$

Since there is no energy consumption in the new defrost method, $\sum \dot{Q}_{input}$ its expression is equal to 0. This method will reduce energy consumption and carbon emissions by $\dot{W}_{resistance}.t_{resistance}$ compared to the electrical resistance defrost method, and by $\dot{W}_{compressor}.t_{compressor,hg}$ compared to the hot gas defrost method.

Uncertainty analysis (W_R) can be calculated using the following equation, considering fixed, random, and manufacturing errors in experimental studies. Where R is the quantity to be measured, the independent variables affecting the R quantity are expressed as x_1, x_2, x_3, …x_n, and the error rates of each independent variable are expressed as w_1, w_2, w_3, …w_n [19]:

$$W_R = \left[\left(\frac{\delta R}{\partial x_1}w_1\right)^2 + \left(\frac{\delta R}{\partial x_2}w_2\right)^2 + \cdots + \left(\frac{\delta R}{\partial x_n}w_n\right)^2\right]^{1/2} \tag{22}$$

Eq. (23) gives the amount of CO_2 emitted per hour (kg CO_2/h). ΦCO_2; the average amount of CO_2 produced in coal, ΨCO_2; emissions show (2.08 kg CO_2/kWh) for the thermal power generation [20]:

$$\phi CO_2 = \psi CO_2 x E_{daily} \tag{23}$$

In the study, an economic analysis calculation was made according to the 25-year economic life of the system and the energy unit price of 0.091 $/kWh. The extra cost of the developed new method compared to conventional defrosting systems was calculated as 146.4$. The equations were used to calculate the amount that would be consumed if conventional systems were used to meet the annual amount of energy required for the defrost event.

$$Q_{def} = P_{def} \times t_{def} \tag{24}$$

$$AC = Q_{def} \times ET \tag{25}$$

$$PP_{def} = \frac{TIC}{AC} \tag{26}$$

In equations (24), (25) and (26), Q_{def} is the energy required for defrosting (kWh), P_{def} is the defrosting power (W), t_{def} is the operating time for the defrosting process, AC is the profit from defrosting ($/year), ET is the unit price of electricity ($/kWh), TIC is the total investment cost ($),$PP_{def}$ is the payback period for the defrosting method (year).

3. Results and discussion

The designed system was tested in November in Ankara in low weather conditions for two 24-hour continuous experiments. Both experiments were started when the two 160 Ah batteries feeding energy to the system reached 100 % charge level. The experiments began at 7:00p.m. and ended at 7:00p.m. the next day. Two experiments (Exp 1 and Exp 2) were out conducted on the cooling system's performance operating according to the automation scenario in 5 different modes in 24-hour hours. Weather conditions graphs of the experiments are given in Fig. 6. During the experiments, an increase was observed in air temperature and solar irradiation values starting from 8:00 a.m. and accordingly 8:00 a.m. accordingly, a decrease was observed in relative humidity levels.

This study observed the temperature change in the cold room while defrosting the cooling system. The temperature change in the cold room during defrosting is given in Fig. 6. As seen in Fig. 7, the temperature

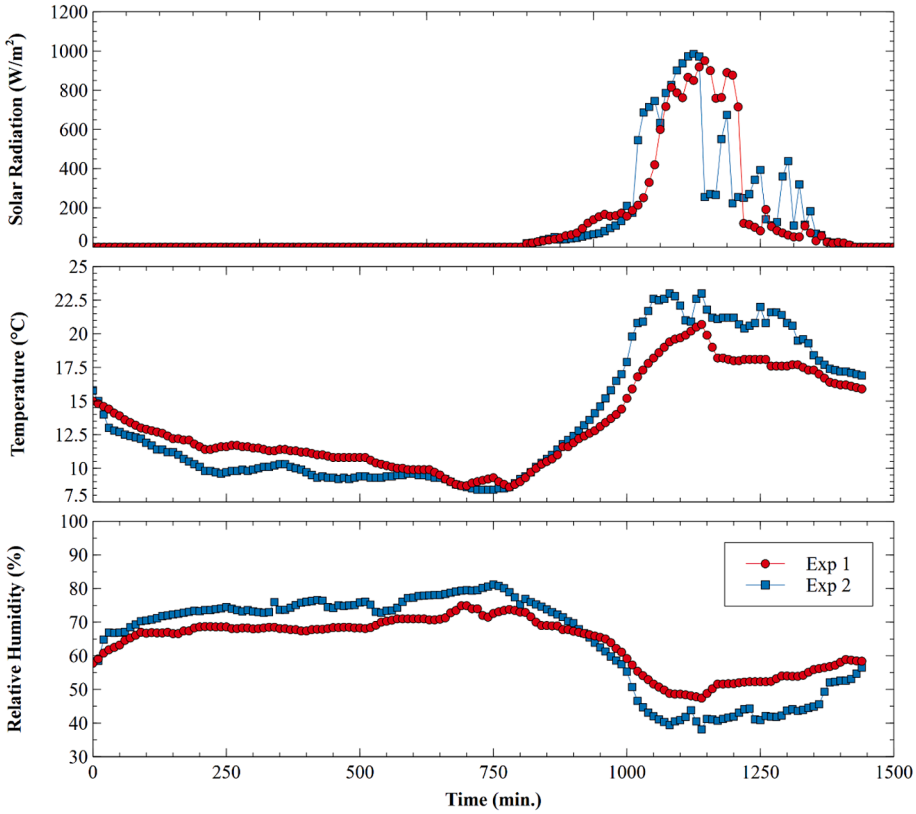

Fig. 6. Solar irradiation, outdoor temperature, and relative humidity values.

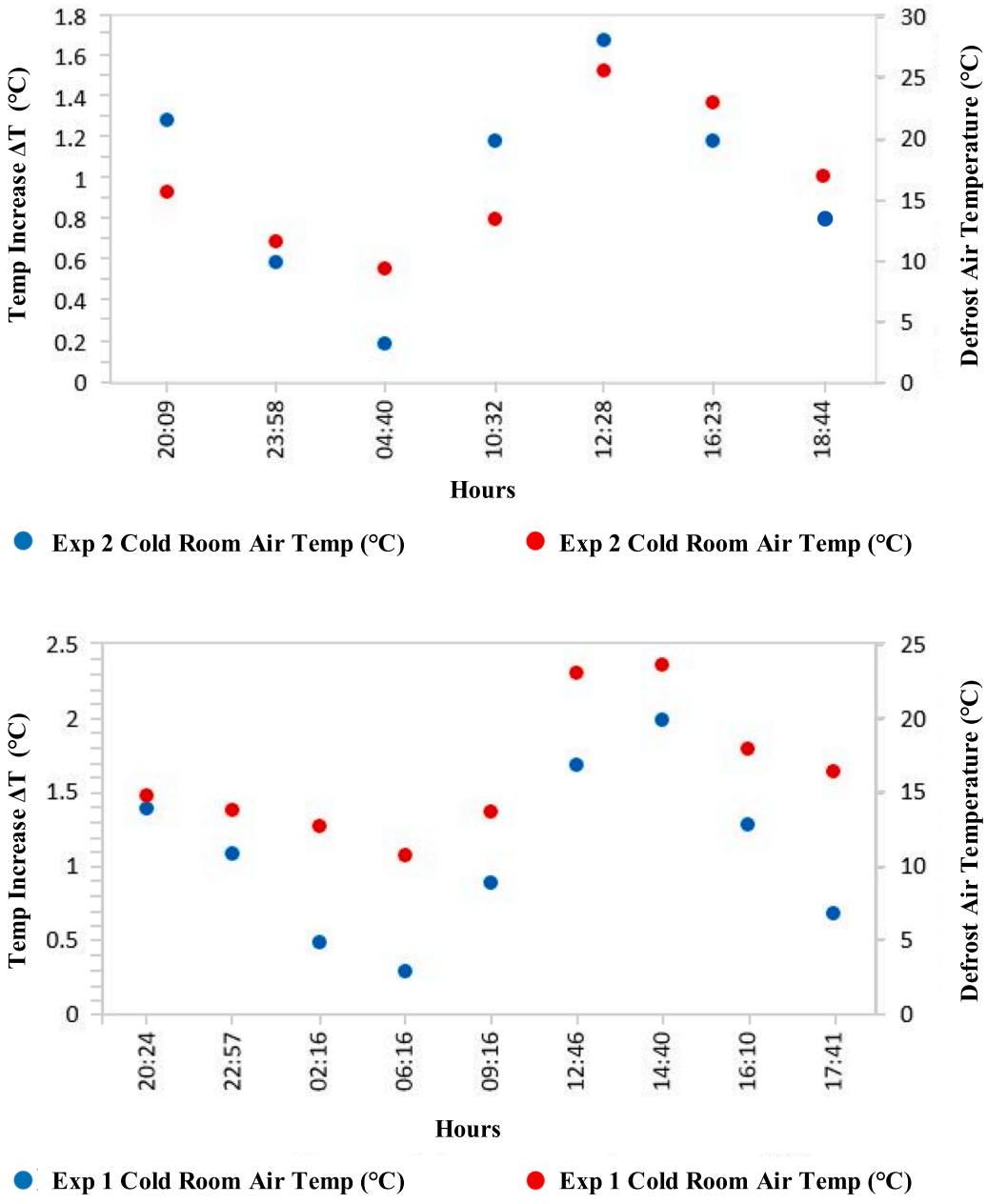

Fig. 7. Temperature change in the cold room during defrosting.

increase in the cold room in Exp 1 was a minimum of 0.3 °C, a maximum of 2 °C, and an average of 1.1 °C, and in Exp 2, a minimum of 0.2 °C, a maximum of 1.7 °C and average of 1 °C. With the proposed cold room design, an energy-efficient system design was achieved in which energy and heat loss were kept at minimum levels.

The times when the system cooling system's compressor started and stopped during the test period are shown in Fig. 8. As a result of the study, as seen in Fig. 8, Exp 1 worked for 584 min in 24 h and became stationary for 856 min. The same situation was observed for Exp 2, which worked for 431 min and remained stationary for 1018 min. It was concluded that when the amount of solar irradiation is high, the start-up time of the compressor is shortened, and the time it stays in operation increases. In Exp 2, due to more cloudiness during the daytime, the hours when the system compressor is on and off are lower than in Exp 1. This caused less energy consumption in Exp 2 and the system remained in regime longer. When starting the experiments, the cold room's initial

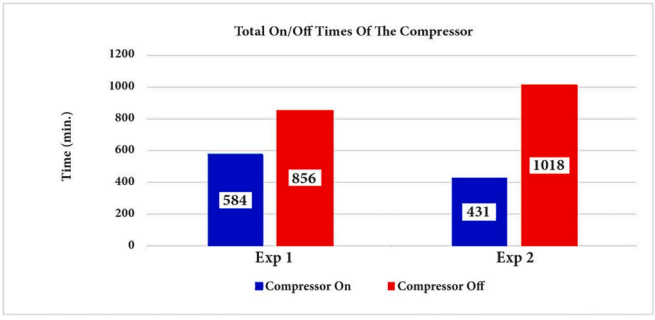

Fig. 8. 24-hour compressor operating status.

temperature value is 18.1 °C in Exp 1 and 10.3 °C in Exp 2. For this reason, Exp 1 remained active for 48 min, and Exp 2 remained active for 22 min at first operation until the temperature of the cold room reached the set value of 4 °C. In both experiments, the compressor continued operating after the cold room temperature entered the regime, as seen in Fig. 8.

The total amount of energy consumed by the system in the 24 h during the automation stages was calculated as 6.25 kWh in Exp 1 and 5.22 kWh in Exp 2. Fig. 9 shows the energy percentages consumed by each scenario in the 5-stage automation scenario in both experiments. In Exp 1, the compressor's operating time was longer in Mode 1 cooling mode. However, in both experiments, Mode 2 PVT cooling mode was activated, but since the irradiation was higher in Exp 1 and the conditions were met, more energy was consumed compared to Exp 2. In addition, while the Mode 3 defrost process occurred nine times in Exp 1, this process occurred seven times in Exp 2. Another automation of the design, in Exp 2 in Mode 5 Standby mode, reached the desired set value of the cold room more quickly and remained in the + 2 °C value band for a longer time. The total energy produced in both experiments was found to be 2.85 kWh in Exp 1 and 2.79 kWh in Exp 2.

This study developed a new PVT-assisted hot air defrosting technique as an alternative to high-consuming energy-consuming methods such as hot gas and electrical resistance. In line with the basic design parameter of our system, assisted by self-sufficient solar energy, a new defrost technique has been developed using waste heat obtained from PVT and a condenser. The heat energy required for defrosting was met by utilizing the waste heat system from the condenser and PVT systems. As a result of both theoretical approaches and experimental results, defrost occurred 9 times in Exp 1 and 7 times in Exp 2 in two 24-hour experiments. In these experiments, 0.945 kWh/24 h and 0.875 kWh/24 h thermal energy (obtained from the solar PVT collector and condenser) was consumed for the defrost process, respectively. As a result of the calculations, if the defrosting process had been carried out under the same ambient conditions as the defrost method with electrical resistance (given in Equation 19–21), our system would have consumed 15.12 % more energy in Exp 1 and 16.76 % more energy in Exp 2.

The CO_2 emissions avoided were calculated with Eq. (23). From an efficiency and environmental point of view when the method investigated in this study was used instead of the traditional electric resistance or hot gas technique, the average annual energy consumption was calculated as 332.15 kWh by multiplying the averages of the energy consumed in the defrosting process for both experiments by 365 days. In addition, extra thermal energy would have been consumed in conventional systems and thus 690.87 kg of CO_2 equivalent emissions per year were prevented. With this proposed method, extra energy consumption in the defrosting process was avoided and energy consumption was reduced by 15.87 % in this research.

Temperature values due to irradiation on the PVT and PV surface during Mode 2 cooling system performance experiments are given in Fig. 10. In Exp 1 and Exp 2, temperature measurements were taken from 5 different points on the surface of PVT and PV. Temperatures were recorded as a result of the test taken in 10-minute periods. Depending on

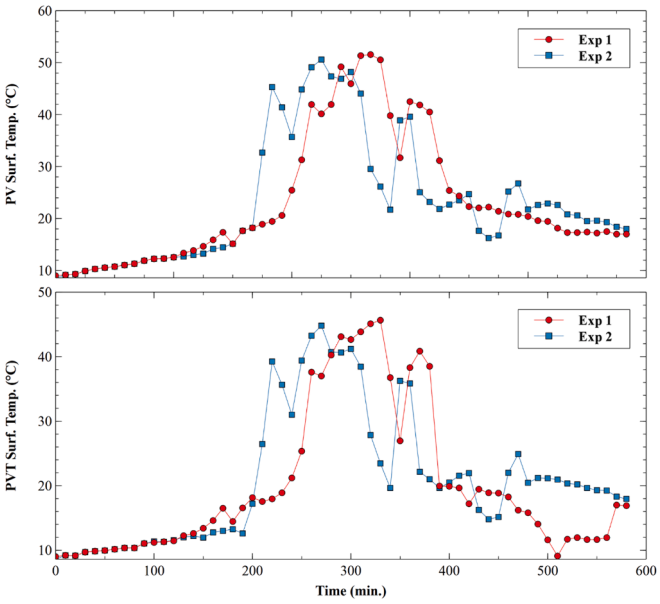

Fig. 10. PVT and PV average surface temperatures.

the average temperature changes, the maximum temperature values for Exp 1 and Exp 2, 45.65 °C and 43.25 °C were measured in PVT and 51.55 °C and 50.06 °C in PV, respectively. As a result of these results, it was seen that the surface temperature values of the designed PVT system were colder than PV panel.

The refrigeration system's performance is partly determined by its coefficient of performance. The average cooling COP values of the proposed system were calculated as 2.29 for Exp 1 and 2.25 for Exp 2. One of the other values is exergy efficiency. Time-dependent exergy values of the system are given in Fig. 11. In Exp 1, while the exergy values varied between 10.2 % – 39.4 %, the average was 25.74 %. In Exp 2, the average was 24.45 % while altering between 9.3 % – 38.7 %. In addition, the average thermal and electrical efficiency values of PVT were determined as 59.47 % and 19.43 % in Exp 1 and 53.65 % and 19.34 % in Exp 2. The uncertainty values were calculated as ± 1.51 % for COP, ±1.96 % for the thermal efficiency of PVT, ±1.65 % for the electrical efficiency of PVT, and ± 0.14 °C for temperature measurements. As can be seen, calculated uncertainty values are within acceptable levels.

The system's main purpose proposed and tested is to obtain a more efficient cooling performance by solving the defrost system, which affects the cooling performance with the heat received from the system. In cases where the heat obtained was not used during defrost, it was used both for storage and to meet the heat need. Thanks to the PVT design, it was observed that the refrigeration cycle works successfully because the refrigerant entering the evaporator in the system absorbed more heat and provided a stable heat source. Since electrical energy is stored in

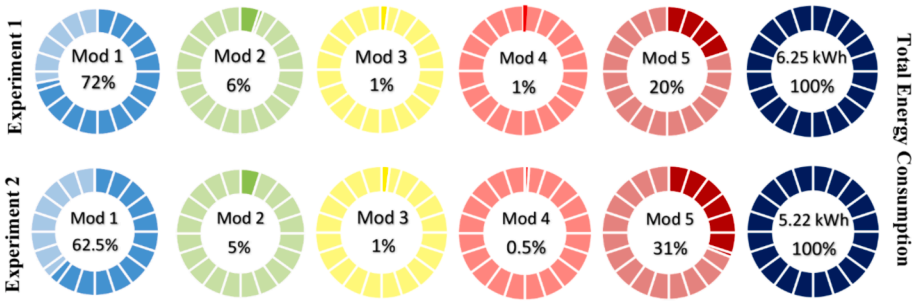

Fig. 9. Energy rates consumed by the system according to modes.

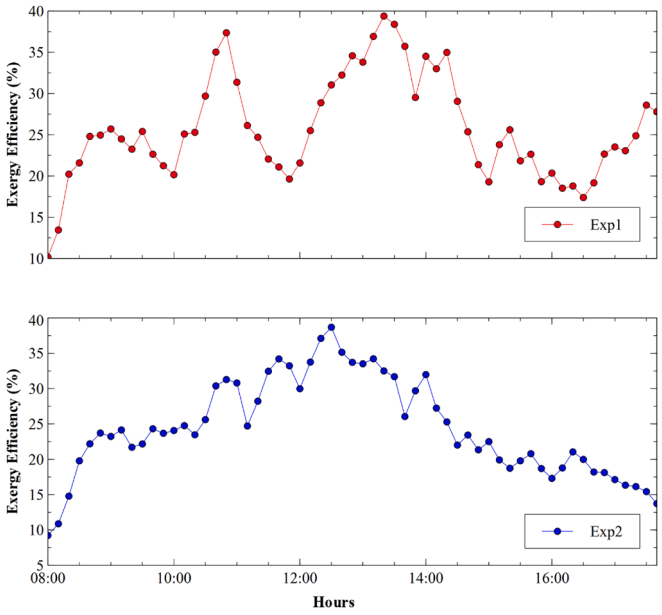

Fig. 11. Exergy efficiency of PVT System.

batteries, the system can meet the necessary heat needs when solar irradiation is insufficient. In addition, the energy consumption required for the defrost process will be prevented at the maximum level. A comparison of the results obtained with similar studies in the literature is presented in Table 2.

According to all research findings, worldwide. Cooling systems and other design models worldwide have many applications. Defrosting is one of the main factors that increase energy consumption in devices serving for cooling purposes. The defrosting process in cooling systems uses classical methods (such as hot gas and electric resistance). When using these methods, electricity consumption increases due to classical methods, temperature increases, and temperature increases in the cold room. Our method, which we have designed, manufactured, and tested, has developed a system that compacts the cooling system with solar energy, generates its energy, and can defrost without consuming extra energy. In the developed method, the evaporator is placed inside the cold room in an external room minimizes the room temperature increase. The rise in room temperature is minimized by suppressing the conditioned air in the cold room during defrosting, thanks to the dampers. Accordingly, a sustainable system design has been developed to defrost without consuming energy.

In the study, an economic analysis calculation was made according to the system's 25-year economic life and 0.091 $/kWh energy unit price. The extra cost of the new method developed compared to conventional defrosting systems was calculated as 146.4$. Since the total amount of energy to be spent for the annual defrosting process was 332.15 kWh/year in conventional methods, the payback period of the system was calculated as 4.84 years. The payback period is shown in Fig. 12.

The complexity of the air flow system management in the proposed new method compared to the classical systems and the sealing of the application at the points where there is air flow may appear as potential obstacles. In addition, the energy used and stored when there is solar irradiation will be in question, and the dependence on the grid or the use of other energy sources when the stored energy runs out when there is no solar radiation can also be expressed as a potential obstacle.

It was investigated that the defrosting process in the cooler integrated in the PVT system can be achieved with hot air from the PVT or condenser and a new air flow structure in the evaporator without heating the cold room during the defrosting process. In this sense, the challenge in the experiments was to ensure very good sealing of the dampers and air ducts in this new approach. The goal of achieving a minimum temperature increase in the cold room during defrosting was prevented by ensuring good sealing in the study. In addition, ensuring the stability of the mechanical system and the automation system to operate successfully in the five different operating modes can also be considered a challenge.Depending on the effects of the findings obtained in the study on the solar-powered cooler providing the extra energy required for defrosting with its own resources, the performance of the system can be improved by developing more rational control systems (supported by artificial intelligence). Efficiency increases in the compressor and fan, which are energy consuming equipment, as well as in the energy generating PVT panel, and the development of rational control applications with advanced technologies will increase efficiency and reduce carbon emissions.

4. Conclusion

This study aimed to bring a new solution to the refrigeration's defrost problem and benefit from maximum solar energy. Therefore, a new PVT-assisted system operating in five different modes was developed. The performance of this proposed system was examined with two 24-hour experiments.

In Exp 1, the compressor operated for 584 min and remained inactive for 856 min, while it operated for 431 min and remained inactive for 1018 min in Exp 2. Moreover, the Mode 3 defrost occurred nine times in Exp 1 and seven times in Exp 2. As a result, 16.48 % less energy was consumed in Exp 2. In the proposed system, the electrical energy was produced from solar energy 2.85 kWh in Experiment 1 and 2.79 kWh in Exp 2.

The average temperature change in the cold room defrosting was observed as 1.1 °C in Exp 1 and 1 °C in Exp 2. In addition, the maximum temperature change of 2 °C was recorded in Exp 1. These temperature increases are reasonable values regarding the cooling technique during the defrost process.

The proposed PVT-assisted refrigeration system's average COP and

Table 2
Comparison of results with other similar studies.

Ref.	Defrost method	Type of study	COP or increase for COP	Exergy efficiency	Temperature increase	Explanation
[21]	Vapor injection defrosting	Experimental	–	–	None	Defrosting time was reduced by 40.48 %, 28.30 % and 23.73 % at − 10 °C, −5°C, and 2 °C.
[22]	Reverse-cycle hot gas defrosting	Experimental	–	–	None	Defrosting time was reduced by 38 %.
[23]	Heat in the liquid line (Sub-cooling)	Experimental	2.23	47.90 %	None	Defrosting efficiency was 100 %.
[24]	Air defrost method	Experimental	2.86	–	3.07 °C (product)	–
[25]	Uninterrupted heating by partial reverse cycle defrosting	Experimental	7 %	–	None	Defrosting time was reduced by 40 %.
This study	PVT assisted and exhausted air	Experimental	2.29 (Exp 1) 2.25 (Exp 2)	25.74 % (Exp 1) 24.45 % (Exp 2)	Min. 0.3 °C – Max. 2 °C (Exp 1), Min. 0.2 °C – Max. 1.7 °C (Exp 2)	Defrosting is off-grid, using the residual heat generated by the system.

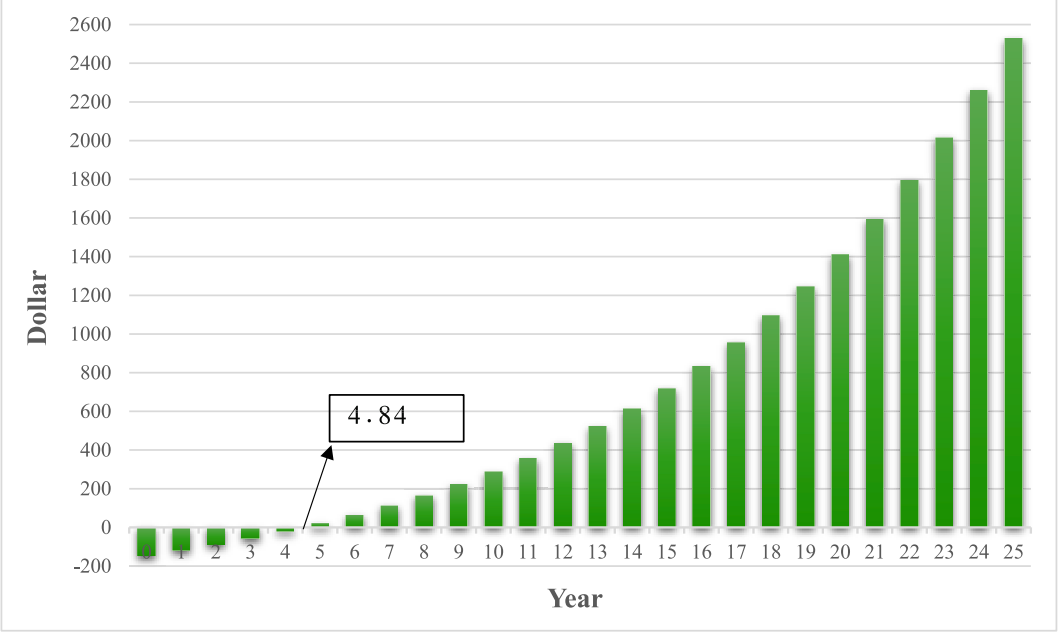

Fig. 12. The payback period of the proposed system.

exergy values were calculated as 2.29 and, 2.25, and 25.74 % and 24.45 %, respectively, in Exp 1 and Exp 2. Compared to the traditional defrosting method, such as electric heaters, this recommended defrosting method does not require high energy consumption or a a long defrosting time.

The effects of the new-generation air flow defrost method with a solar-assisted system were investigated. A compact cooler that can defrost without consuming extra energy by managing the solar energy source and air flow structure has been developed. It has been observed that this proposed system can operate efficiently even when there is no solar irradiation. As a result, a new sustainable, energy-efficient design that will eliminate the problems in the defrost processes of refrigeration systems has been introduced to the literature.

CRediT authorship contribution statement

Burak Aktekeli: Writing – original draft, Methodology, Data curation, Conceptualization. **Mustafa Aktaş:** Writing – review & editing, Validation, Supervision, Conceptualization. **Meltem Koşan:** Writing – review & editing, Writing – original draft, Investigation, Conceptualization. **Yaren Güven:** Writing – original draft, Methodology, Investigation, Writing – review & editing. **Erhan Arslan:** Validation, Formal analysis, Data curation.

Declaration of competing interest

The authors declare that they have no known competing financial interests or personal relationships that could have appeared to influence the work reported in this paper.

Data availability

No data was used for the research described in the article.

Acknowledgements

Gazi University for their contributions to the study of the University Scientific Research Projects Coordination Unit (Project Code: FDK-2022-7868) is gratefully acknowledged. We would also like to acknowledge Nurdil Refrigeration Inc. and FZL Engineering. We would like to thank them for their contribution.

References

[1] G. Milev, A. Al-Habaibeh, S. Fanshawe, F.L. Siena, Investigating the Effect of the Defrost Cycles of Air-Source Heat Pumps on Their Electricity Demand in Residential Buildings, Energy and Buildings 300 (2023) 113656, https://doi.org/10.1016/j.enbuild.2023.113656.
[2] X. Qiao, X. Kong, H. Li, L. Wang, H. Long, Performance and Optimization of A Novel Active Solar Heating Wall Coupled with Phase Change Material, Journal of Cleaner Production 250 (2020) 119470, https://doi.org/10.1016/j.jclepro.2019.119470.
[3] Z.L. Li, C.L. Zhang, H.M. Liu, X.C. Wang, Feasibility Analysis of Thermal Storage Defrosting Method for Air Source Heat Pump: From Energetic and Economic Viewpoints, Applied Thermal Engineering 236 (2024) 121828, https://doi.org/10.1016/j.applthermaleng.2023.121828.
[4] F.T. Knabben, C.J.L. Hermes, C. Melo, In-situ study of frosting and defrosting processes in tube-fin evaporators of household refrigerating appliances, International Journal of Refrigeration 34 (8) (2011) 2031–2041, https://doi.org/10.1016/j.ijrefrig.2011.07.006.
[5] H. Tan, T. Xu, Z. Liu, T. Tao, G. Xu, Investigation of ultrasonic array defrosting method based on synergism of standing wave intermittent phase-stagger and multi-frequency for finned-tube evaporator, Energy and Buildings 218 (2020) 110054, https://doi.org/10.1016/j.enbuild.2020.110054.
[6] M.O. Karaağaç, A. Ergün, A.E. Gürel, İ. Ceylan, G. Yıldız, Assessment of A Novel Defrost Method for PVT System Assisted Sustainable Refrigeration System, Energy Conversion and Management 267 (2022) 115943, https://doi.org/10.1016/j.enconman.2022.115943.
[7] A.N. Malik, S.A. Khan, İ. Lazoğlu, A Novel Hybrid Frost Detection and Defrosting System for Domestic Refrigerators, International Journal of Refrigeration 117 (2020) 256–268, https://doi.org/10.1016/j.ijrefrig.2020.05.016.
[8] Y. Yoon, H. Jeong, K.S. Lee, Adaptive Defrost Methods for Improving Defrosting Efficiency of Household Refrigerator, Energy Conversion and Management 157 (2018) 511–516, https://doi.org/10.1016/j.enconman.2017.12.039.
[9] X. Yu, S. Jiang, S. Zhang, Energy, Exergy, Economic and environmental Assessment of Solar Photovoltaic Direct-Drive Refrigeration System for Electronic Device Cooling, Renewable Energy 129 (2023) 119538, https://doi.org/10.1016/j.renene.2023.119538.
[10] J. Klingebiel, M. Hassan, V. Venzik, C. Vering, D. Müller, Efficiency Comparison Between Defrosting Methods: A Laboratory Study on Reverse-Cycle Defrosting, Electric Heating Defrosting, and Warm Brine Defrosting, Applied Thermal Engineering (2023) 121072, https://doi.org/10.1016/j.applthermaleng.2023.121072.
[11] H. Miao, X. Yang, D. Yin, W. Zheng, H. Zhang, S. Zhang, Z. Liu, A Novel Defrosting Control Strategy with Image Processing Technique and Fractal Theory, International Journal of Refrigeration 138 (2022) 259–269, https://doi.org/10.1016/j.ijrefrig.2022.03.002.
[12] A.A. Ammar, K. Sopian, M.A. Alghoul, B. Elhub, A.M. Elbreki, Performance study on photovoltaic/thermal solar-assisted heat pump system, Journal of Thermal Analysis and Calorimetry 136 (2019) 79–87, https://doi.org/10.1007/s10973-018-7741-6.

[13] A. Kazemian, A. Taheri, A. Sardarbadi, M. Tao, M. Passandideh-Fard, J. Peng, Energy, exergy and environmental analysis of glazed and unglazed PVT system integrated with phase change material: An experimental approach, Sol. Energy 201 (2020) 178–189, https://doi.org/10.1016/j.solener.2020.02.096.
[14] M. Koşan, M. Demirtaş, M. Aktaş, M. Dişli, Performance analyses of sustainable PVT assisted heat pump drying system, Solar Energy 199 (2020) 657–672, https://doi.org/10.1016/j.solener.2020.02.040.
[15] M.D. Dashtebayaz, S.V. Namanlo, Thermoeconomic and environmental feasibility of waste heat recovery of a data center using air source heat pump, J. Clean. Prod. 219 (2019) 117–126, https://doi.org/10.1016/j.jclepro.2019.02.061.
[16] M. Koşan, M. Aktaş, Experimental investigation of a novel thermal energy storage unit in the heat pump system, Journal of Cleaner Production 311 (2021) 127607, https://doi.org/10.1016/j.jclepro.2021.127607.
[17] J. Liang, L. Sun, T. Li, A novel defrosting method in gasoline vapor recovery application, Energy 163 (2018) 751–765, https://doi.org/10.1016/j.energy.2018.08.172.
[18] M. Koşan, E. Arslan, S. Erten, F.N. Erdoğmuş, M. Aktaş, Determination of defrost efficiency and energy efficiency index value using different defrost methods and refrigerants: An experimental study, Science and Technology for the Built Environment 28 (2022) 1012–1023, https://doi.org/10.1080/23744731.2022.2076504.
[19] E.K. Akpınar, Drying of mint leaves in a solar dryer and under open sun: Modelling performance analyses, Energy Con, Manag. 51 (12) (2010) 2407–2418, https://doi.org/10.1016/j.enconman.2010.05.005.
[20] R. Tripathi, V. Tiwari, V. Dwivedi, Overall energy, exergy and carbon credit analysis of n partially covered photovoltaic thermal (PVT) concentrating collector connected in series, Solar Energy 136 (2016) 260–267, https://doi.org/10.1016/j.solener.2016.07.002.
[21] M. Lin, Y. Song, L. Wu, L. Ni, Experimental investigation on vapor injection defrosting performance of quasi-two-stage compression air source heat pump with flash tank, Applied Thermal Engineering 244 (2024) 122601, https://doi.org/10.1016/j.applthermaleng.2024.122601.
[22] H. Wenju, J. Yiqiang, Q. Minglu, N. Long, Y. Yang, D. Shiming, An experimental study on the operating performance of a novel reverse-cycle hot gas defrosting method for air source heat pumps, Applied Thermal Engineering 31 (2011) 363–369, https://doi.org/10.1016/j.applthermaleng.2010.09.024.
[23] M.O.A. Abdullah, E. Deniz, M. Karagöz, G. Gürüf, An experimental study on a novel defrosting method for cold room, Applied Thermal Engineering 188 (2021) 116573, https://doi.org/10.1016/j.applthermaleng.2021.116573.
[24] S. Erten, M. Koşan, F. İşgen, M. Aktaş, Experimental Analysis of the Air Defrost Process in An Industrial Cooling System, Journal of Scientific Reports-A 45 (2020) 143–157. https://dergipark.org.tr/en/pub/jsr-a/issue/59227/851282.
[25] L. Tang, X. Liu, S. He, Q. Li, Performance of an air-source heat pump with multi-circuit outdoor coil for continuous heating during defrosting, Journal of Building Engineering 45 (2024) 108739, https://doi.org/10.1016/j.jobe.2024.108739.